Scientific Research Publishing

Open Journal of Energy Efficiency, 2024, 13, 101-119
https://www.scirp.org/journal/ojee
ISSN Online: 2169-2645
ISSN Print: 2169-2637

Mutual Coupling Effect on Spectral Efficiency of 5G Massive MIMO Millimeter Wave Antenna Array

Ezeddin A. M. Ben Ihrayz[1,2]

[1]Department of Electrical and Electronic Engineering, Faculty of Engineering, University of Benghazi, Benghazi, Libya
[2]Hatif Libya Company, Benghazi, Libya
Email: ez1161972@yahoo.com, ez1161972@gmail.com

How to cite this paper: Ben Ihrayz, E.A.M. (2024) Mutual Coupling Effect on Spectral Efficiency of 5G Massive MIMO Millimeter Wave Antenna Array. *Open Journal of Energy Efficiency*, **13**, 101-119.
https://doi.org/10.4236/ojee.2024.134007

Received: August 27, 2024
Accepted: October 11, 2024
Published: October 14, 2024

Abstract

The fifth generation (5G) wireless communication requires the massive multiple input multiple output (MIMO) technique. The massive MIMO antenna array of the millimeter wave (mm-wave) is recognized as a key enabler because of its high spectral efficiency. The higher the frequencies of the RF signal, the lower the distance it travels in free space caused by path loss, and it is more easily absorbed by obstacles, which are needed for high-gain transmitters. The advantage of the physical properties of higher New Radio (NR) frequencies is that 5G can utilize more spectrum, more antennas, and higher-order modulation schemes. The massive antennas and radio frequency chains improve the implementation of the cost of 5G wireless communication systems and result in an intense mutual coupling effect among antennas because of the limited space for deploying antennas. The upper bound of the effective capacity is derived for 5G multimedia massive MIMO communication systems. Two antennas that receive diversity gain models, the mutual coupling matrix, and the spacing antenna distance are built and analyzed. The impacts and affections of the antenna spacing the number of antennas, the quality-of-service (QoS) statistical exponent, and the number of independent incident directions on the upper effective capacity of 5G multimedia massive MIMO communication systems are analyzed. It is shown that for MIMO systems with compact transmit antenna arrays, the mutual coupling seriously degrades system capacity to mitigate the capacity degradation. In case of improvement in the mutual coupling by 99%, the system performance is kept stationary and enhances system capacity. However, the improvement of the mutual coupling is still about 87.5% today, which means the mutual coupling should be considered in 5G massive MIMO networks.

Keywords

Mutual Coupling, Antenna Array, Massive MIMO, Spectral Efficiency, Effective Capacity, Multiuser, Multipath Directions, Scattering Matrix, Steering Matrix

1. Introduction

The exact extent nature of the effects of coupling on array performance depends on the type of antenna, its design parameters, the relative placement of the element in the array, the type of feed used to excite elements and design parameters thereof, and the range of relative excitation employed [1] [2]. To support this large data traffic 5G is the latest possible solution. For 5G, frequencies of around 50 GHz are being considered, which will present some real challenges in the circuit design [3]. A Multiple-Input Multiple-Output (MIMO) antenna system can enhance the overall antenna performance but has to overcome new challenges, such as reducing the mutual coupling and the correlation between the elements [4] [5]. The huge antenna arrays have to be deployed compactly because enough spaces are not available at not only base stations (BSs) but also mobile terminals; therefore, the interaction of mutual coupling among antennas gets so strong that it cannot be ignored in massive MIMO systems [6]. It has been proved that mutual coupling has a great influence on the performance of antenna arrays for not only small but also large inter-antenna spacing, because in order to contain the changes in all the anticipant vectors, the steering vectors of the antenna arrays should be adjusted not only in amplitude but also in phase [6] [7].

The motivation rest of this paper produces the system model in which there is a 2D antenna array is described for a massive MIMO mobile communication system, mutual coupling impedance, diversity gain for antenna spacing, antenna number diversity gain, optimal precoding matrix, upper bound of spectral efficiency is derived, and effective capacity with (QoS) quality-of-service statistical exponent. Numerical analysis is performed using the MATLAB program, and comments on the results of the mutual coupling effect of the massive MIMO modeling are summarized in this paper.

2. System Model

2.1. Downlink 2D (Two Dimension) Massive MIMO Communication system

Multiple input multiple output communication mobile, with multiple paths scattering environment system, are shown in **Figure 1**. In the beginning, the massive MIMO (Multiple Input Multiple Output) parameters of the system model are explained.

Definition λ as the wavelength of the carrier signal, d as the antenna spacing distance between adjacent elements of the antenna array of the massive MIMO, $a\lambda$ ($a \geq 1$) as the length of the antenna array, $b\lambda$ ($b \geq 1$) as the width of the antenna

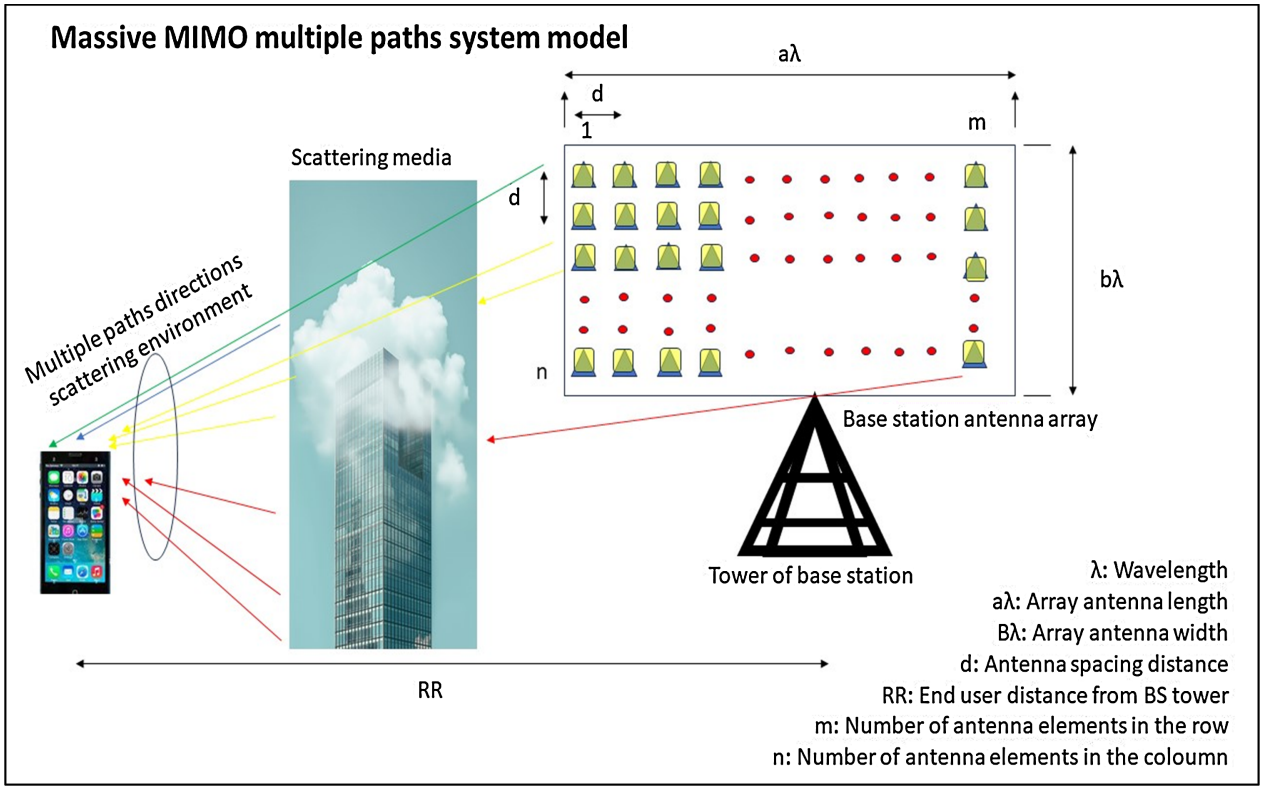

Figure 1. Massive MIMO multiple path system model.

array, deployment of m antenna elements in each row, and n elements in each column of this antenna array. The total number of elements, M of the antenna array of the massive MIMO (Multiple Input Multiple Output) can be derived as follows [6].

$$M = m * n \tag{1}$$

The signal-to-noise ratio at the base station is noted as SNR_{BS}. $\boldsymbol{H}$, and β stand for the small-scale fading matrix, and large-scale fading coefficient of the channel in this model respectively. The signal at the base station (BS) is defined as $\boldsymbol{x}$, $\boldsymbol{w}$ means the additive white Gaussian noise (AWGN) over wireless channels, and the mutual coupling matrix is configured as $\boldsymbol{K}$, the equivalent precoding matrix is recognized as $\boldsymbol{F}_{eq}$, $\boldsymbol{A}$ is defined as the steering matrix, then the down-link signal vector received at the user end (UE) mobile terminal equipped with $\boldsymbol{N}$ antenna at the receiver can be expressed as follows [5] [6].

$$\boldsymbol{y} = \sqrt{SNR_{BS}}\boldsymbol{HAKF}_{eq}\beta^{1/2}\boldsymbol{x} + \boldsymbol{w} \tag{2}$$

In which $\boldsymbol{x}$, is as a $N_s \times 1$ vector, and $\boldsymbol{w}$ is a $N \times 1$ vector, where N_s is the number of data streams received at the received antenna, and N is the number received antenna at the mobile terminal of the user end (UE).

The scattering matrix $\boldsymbol{H} \sim \mathcal{CN}(0, P\boldsymbol{I})$ is governed by a complex Gaussian distribution and is expressed as follows.

$$\boldsymbol{H} = \left[h_1, \cdots, h_p, \cdots, h_P\right]^{\mathrm{T}} \in \mathbb{C}^{N \times P} \tag{3}$$

In which $\mathbb{C}^{N\times P}$ denotes a $N\times P$ matrix of a complex number, P stands for the number of independent incident directions from scattering media environment. $h_p \sim \mathcal{CN}(0,I)$ stands for a complex coefficient vector of small-scale fading from the p_{th} incident direction scattering media environment which is expressed as follows.

$$h_p = h_p^{(r)} + h_p^{(i)} \tag{4}$$

The above-mentioned expression consists $h_p^{(r)}$ is defined as a real part of h_p, and $h_p^{(i)}$ is defined as an imaginary part of h_p. Furthermore, they are Gaussian random variables distributed independently and identically, whose expectation, and variance are 0 and 0.5 respectively [6].

The expectation of a random variable is defined as a mean value as mentioned in [8] as follows.

$$E[X] = \int_{-\infty}^{\infty} x \cdot f(x)\mathrm{d}x \tag{5}$$

where $E[X]$ is the expectation of a random variable X, $f(x)$ distribution function of a random variable, and x ranges over all possible realization of X [8].

$$\mathrm{var}(X) = E\left[\left(X - E[X]\right)^2\right] = E\left[X^2\right] - E[X]^2 \tag{6}$$

where $\mathrm{var}(X)$ is the variance of the random variable, $E\left[X^2\right]$ is called the second moment of a random variable or mean square of the random variable and is given by [8].

$$E\left[X^2\right] = \int_{-\infty}^{\infty} x^2 f(x)\mathrm{d}x \tag{7}$$

The standard deviation σ_x is defined as the root square of the variance as follows [8].

$$\sigma_x = \sqrt{\mathrm{var}(X)} \tag{8}$$

Each independent incident direction corresponds to one steering vector $a(\phi_q,\theta) \in \mathbb{C}^{M\times 1}$, so all the P steering vectors can constitute the steering matrix $\boldsymbol{A}$ of the antenna array, which is expressed as follows. Here assuming both azimuth angle $\phi_q\,(q = 1,2,\cdots,P)$, and elevation angle θ, which are uniform distributed independently and identically within scope of $[-\pi/2,\pi/2]$,

$$\boldsymbol{A} = \left[a(\phi_1,\theta), a(\phi_2,\theta), \cdots, a(\phi_q,\theta), \cdots, a(\phi_P,\theta)\right]^{\mathrm{T}} \in \mathbb{C}^{P\times M} \tag{9}$$

The steering matrix of q_{th} incident independent direction of the rectangular antenna array is defined by $\boldsymbol{A}^q \in \mathbb{C}^{n\times m}$ [6].

$$\mathrm{vec}\left(\boldsymbol{A}^q\right) = a(\phi_q,\theta) \tag{10}$$

where $\mathrm{vec}\left(\boldsymbol{A}^q\right)$ is defined as a vectorization matrix operation [9]. Which is defined as below.

$$\mathrm{vec}\left(\boldsymbol{A}^q\right) = \left[a_{1,1}, a_{2,1}, \cdots, a_{n,1}, \cdots, a_{1,2}, a_{2,2}, \cdots, a_{n,2}, \cdots, a_{1,m}, a_{2,m}, \cdots, a_{n,m}\right]^{\mathrm{T}} \tag{11}$$

where $[\,]^T$ transpose matrix operation [6] [9].

The definition element of steering matrix of A^q as below.

$$A_{ce}^{q} = \exp\left\{ j\frac{2\pi}{\lambda}\left[(c-1)d\cos\phi_q \sin\theta + (e-1)d\sin\phi_q \sin\theta \right] \right\} \tag{12}$$

where $A_{ce}^{q}\left(1 \le c \le m, 1 \le e \le n\right)$ is the element of the steering matrix A^q.

Which locates at cth row, and eth column [5] [6].

For a rectangular antenna array with M elements the mutual coupling matrix is defined and expressed as below [6].

$$\boldsymbol{K} = Z_L \left(Z_L \boldsymbol{I} + \boldsymbol{Z}_M \right)^{-1} \tag{13}$$

where Z_L denotes the antenna load impedance that is constant for each element of the antenna array equal to 50 Ω, $\boldsymbol{Z}_M$ denotes the $M \times M$ mutual coupling impedance matrix, and $\boldsymbol{I}$ is the $M \times M$ unity matrix [6] [10].

2.2. Mutual Coupling Effect Modeling

The induced EMF (Electro Motive Force) method is a classical method to compute the self and mutual impedances [6]. The coupling between two or more microstrip antenna elements can be taken into account easily, and it can be shown that coupling between two patches, as is coupling between two aperture or two wire antennas, is a function of the position of one element relative to the other [11] [12]. This has been demonstrated in a vertical half-wavelength dipole above a ground plane, and in a horizontal half-wavelength dipole above a ground plane. From these two, the ground effects are more pronounced for the horizontal dipole.

The general expression of the induced electro-motive force developed by Carter has been the most widely used procedure for determining mutual coupling impedance between linear array elements of equal length h and a spacing distance d between two adjacent elements, which is expressed below [11]-[14].

$$\begin{aligned} R_{21} = \frac{\eta}{4\pi}\Big(& \sin(kh)\cos(kh)\left[S_i(u_2) - 2S_i(v_1) - S_i(v_2) + 2S_i(u_1) \right] \\ & - \frac{\cos(2kh)}{2}\left[2C_i(u_1) - 2C_i(u_0) + 2C_i(v_1) - C_i(u_2) - C_i(v_2) \right] \\ & - \left[C_i(u_1) - 2C_i(u_0) + C_i(v_1) \right] \Big) \end{aligned} \tag{14}$$

$$\begin{aligned} X_{21} = \frac{-\eta}{4\pi}\Big(& \sin(kh)\cos(kh)\left[2C_i(v_1) - 2C_i(u_1) + C_i(v_2) - C_i(u_2) \right] \\ & - \frac{\cos(2kh)}{2}\left[2S_i(u_1) - 2S_i(u_0) + 2S_i(v_1) - S_i(u_2) - S_i(v_2) \right] \\ & - \left[S_i(u_1) - 2S_i(u_0) + S_i(v_1) \right] \Big) \end{aligned} \tag{15}$$

where R_{21} is the real part of the mutual impedance (resistance) between two elements, X_{21} is the imaginary part of the mutual impedance (reactance), $C_i(x)$ is the Cosine integral, and $S_i(x)$ is the Sine integrals, which both are given by [11]-[14].

$$S_i(x) = \int_0^x \frac{\sin(y)}{y} \mathrm{d}y \tag{16}$$

$$C_i(x) = -\int_x^{\infty} \frac{\cos(y)}{y} \mathrm{d}y \tag{17}$$

$$C_{in}(x) = 0.5772 + \ln(x) - C_i(x) \tag{18}$$

$$C_{in}(x) = \int_0^x \frac{1-\cos(y)}{y} \mathrm{d}y \tag{19}$$

$$\int_0^x \frac{\sin(y)}{y} \mathrm{d}y = x - \frac{x^3}{3\times 3!} + \frac{x^5}{5\times 5!} - \frac{x^7}{7\times 7!} + \cdots \tag{20}$$

$$C_{in}(x) = \frac{X^2}{2\times 2i} - \frac{X^4}{4\times 4i} + \frac{X^6}{6\times 6i} - \frac{X^8}{8\times 8i} + \cdots \tag{21}$$

Other parameters of mutual coupling impedance are noted below.

$$u_0 = kd \tag{22}$$

$$u_1 = k\left(\sqrt{d^2 + h^2} - h\right) \tag{23}$$

$$u_2 = k\left(\sqrt{d^2 + (2h)^2} + 2h\right) \tag{24}$$

$$v_1 = k\left(\sqrt{d^2 + h^2} + h\right) \tag{25}$$

$$v_2 = k\left(\sqrt{d^2 + (2h)^2} - 2h\right) \tag{26}$$

$$k = \omega\sqrt{\mu\varepsilon} \tag{27}$$

where η is the intrinsic impedance, which is equal to $\eta = 120\pi = 377\ \Omega$, h is the equivalent dipole dimension or dipole length, which is equal to $h = 0.5\lambda$, d is the antenna spacing distance, ω is the radian frequency equal to $\omega = 2\pi f = 2\pi\left(3\times 10^8\right)/\lambda$, μ is the permeability of the medium which is equal to $4\pi \times 10^{-7}$ H/m of vacuum medium, ε is the permittivity of the medium, which is equal to 8.854×10^{-12} F·m^{-1} of vacuum medium, f and λ Are frequency and wavelength of the carrier signal respectively. In the case of vacuum medium or air medium, the parameter of k in Equation (27) is equal to $k \approx 2\pi/\lambda$ [11]-[14].

The mutual impedance matrix $\boldsymbol{Z}_M$ can be constructed by $n \times n$ sub-matrices that is $\boldsymbol{Z}_M = [\boldsymbol{Z}_{st}]_{n\times n}$, where $\boldsymbol{Z}_{st}$, as an $m \times m$ mutual impedance sub-matrix, denotes the mutual impedance between m antennas located at sth ($s = 1, 2, \cdots, n$) row and the m antennas located at tth ($t = 1, 2, \cdots, n$) column in the rectangular antenna array [6]. For ease of exposition, the definition of Ant_{su} as the antenna located at the sth row, and uth column ($s = 1, 2, \cdots, m$; $u = 1, 2, \cdots, m$) of the rectangular antenna array. And the definition of Ant_{tv} as the antenna located at tth row, and vth column ($t = 1, 2, \cdots, m$; $v = 1, 2, \cdots, m$) of the rectangular antenna array, the corresponding distance between which is given by Equation (28) as follows [6].

$$d_{uv}^{st} = d\sqrt{(t-s)^2 + (v-u)^2} \tag{28}$$

Thus, sub-matrices $\boldsymbol{Z}_{st}$, can be written as follows.

$$\boldsymbol{Z}_{st} = \begin{bmatrix} z_{11}^{st} & z_{12}^{st} & z_{13}^{st} & \cdots & z_{1m}^{st} \\ z_{21}^{st} & z_{22}^{st} & z_{23}^{st} & \cdots & z_{2m}^{st} \\ \vdots & \vdots & \vdots & \ddots & \vdots \\ z_{m1}^{st} & z_{m2}^{st} & z_{m3}^{st} & \cdots & z_{mm}^{st} \end{bmatrix} \tag{29}$$

Then the mutual coupling impedance z_{uv}^{st} between two elements, which are separated by distance of d_{uv}^{st} can be obtained by using Equation (14) through up to Equation (29). The mutual coupling matrix $\mathrm{Z_M}$ can be derived by sub-matrix of $\boldsymbol{Z}_{st}$ construction as follows.

$$\boldsymbol{Z}_{M} = \begin{bmatrix} \boldsymbol{Z}_{11} & \boldsymbol{Z}_{12} & \boldsymbol{Z}_{13} & \cdots & \boldsymbol{Z}_{1n} \\ \boldsymbol{Z}_{21} & \boldsymbol{Z}_{22} & \boldsymbol{Z}_{23} & \cdots & \boldsymbol{Z}_{2n} \\ \vdots & \vdots & \vdots & \ddots & \vdots \\ \boldsymbol{Z}_{n1} & \boldsymbol{Z}_{n2} & \boldsymbol{Z}_{n3} & \cdots & \boldsymbol{Z}_{nn} \end{bmatrix} \tag{30}$$

There are some properties, which are mentioned in [6]. The advantage of properties is that the computational complexity can be significantly reduced compared with direct calculation of the $M \times M$ entries of $\boldsymbol{Z}_M$, especially with a large M. mutual coupling matrix as mentioned in Equation (13) can be constructed, when mutual coupling impedance is known, and built as mentioned in Equation (14) to Equation (30).

3. The Equivalent Precoding Matrix.

The equivalent precoding matrix $\boldsymbol{F}_{eq} = \boldsymbol{F}_{BB} \times \boldsymbol{F}_{RF}$ consists of the baseband precoding matrix $\boldsymbol{F}_{BB}$, and the RF precoding matrix $\boldsymbol{F}_{RF}$. The optimal precoding matrix is derived by SVD method [5] [6].

$$\boldsymbol{F}_{eq} = \boldsymbol{U}_F \boldsymbol{\Sigma}_F \boldsymbol{V}_F^{TC} \tag{31}$$

In which $\boldsymbol{U}_F$, and $\boldsymbol{V}_F^{TC}$ are unitary matrices. When the SVD (singular value decomposition) method is performed by using MATLAB over the equivalent channel $\boldsymbol{H}_{eq}$, which is equal to multiplying small-scale fading matrix by steering matrix and by mutual coupling matrix. The $\boldsymbol{V}_F^{TC}$ is noted as a conjugate transpose of $\boldsymbol{V}_F$.

$$\boldsymbol{H}_{eq} = \boldsymbol{HAK} \tag{32}$$

The equivalent channel matrix is derived by [5] [6].

$$\boldsymbol{H}_{eq} = \boldsymbol{U}_H \boldsymbol{\Sigma}_H \boldsymbol{V}_H^{TC} \tag{33}$$

With

$$\boldsymbol{\Sigma}_H = \begin{pmatrix} \boldsymbol{\Delta}_H & \boldsymbol{0} \\ \boldsymbol{0} & \boldsymbol{0} \end{pmatrix} \tag{34}$$

$$\boldsymbol{\Delta}_H = \begin{bmatrix} \gamma_1 & 0 & 0 & \cdots & 0 \\ 0 & \gamma_2 & 0 & \cdots & 0 \\ 0 & 0 & \gamma_3 & \cdots & 0 \\ \vdots & \vdots & \vdots & \ddots & \vdots \\ 0 & 0 & 0 & \cdots & \gamma_r \end{bmatrix} \tag{35}$$

In which $\boldsymbol{U}_H$ and $\boldsymbol{V}_H^{TC}$ are unitary matrices, that implies $\boldsymbol{U}_H\boldsymbol{U}_H^{TC}=\boldsymbol{I}$ and $\boldsymbol{V}_H\boldsymbol{V}_H^{TC}=\boldsymbol{I}$ where $\boldsymbol{I}$ is the unity matrix.

In which $\boldsymbol{\Sigma}_{\mathrm{F}}$ is noted bellow.

$$\boldsymbol{\Sigma}_F=\begin{pmatrix}\boldsymbol{\Delta}_F & \boldsymbol{0}\\ \boldsymbol{0} & \boldsymbol{0}\end{pmatrix} \tag{36}$$

$$\boldsymbol{\Delta}_F=\begin{bmatrix} f_1 & 0 & 0 & \cdots & 0\\ 0 & f_2 & 0 & \cdots & 0\\ 0 & 0 & f_3 & \cdots & 0\\ \vdots & \vdots & \vdots & \ddots & \vdots\\ 0 & 0 & 0 & \cdots & f_r\end{bmatrix} \tag{37}$$

where r is the rank of scattering fading channel matrix $\boldsymbol{H}$, $r=rank(\boldsymbol{H})$. Assume the transmission power at the base station (BS) is independent of the equivalent precoding matrix. This assumption implies that $\left\|\boldsymbol{F}_{eq}\right\|=N_s$, where the operator $\|\|$ is the norm operation of the equivalent precoding matrix [9], that is.

$$\sum_{i=1}^{r} f_i^2=N_s^2 \tag{38}$$

Which is mentioned in [6]. Based on Equation (38), the square of eigenvalues at the equivalent precoding matrix $\boldsymbol{F}_{eq}$ is derived by the following:

$$f_i^2=\frac{N_s\left(\frac{1}{\gamma_1^2}+\frac{1}{\gamma_2^2}+\cdots+\frac{1}{\gamma_r^2}\right)}{rSNR_{BS}}+\frac{N_s^2}{r}-\frac{N_s}{SNR_{BS}\gamma_i^2} \tag{39}$$

In this case the equivalent precoding matrix is simplified as follows.

$$\boldsymbol{F}_{eq}=\boldsymbol{V}_H\boldsymbol{\Sigma}_F \tag{40}$$

Based on the method in [15], the optimal precoding matrix $\boldsymbol{F}_{eq}$ is composed of $\boldsymbol{F}_{RF}$ and $\boldsymbol{F}_{BB}$, which are designed in [6] [15].

4. Receive Diversity Gain Models

Deployed in a constrained space at the BS, the number of antenna elements is inversely proportional to the antenna spacing, that is, a larger number of antennas leads to a smaller antenna spacing [6]. More antennas lead to a higher receive diversity gain of the massive MIMO system, whereas the diversity gain can be compromised by the mutual coupling effect that is caused by decreasing the antenna spacing. Thus, when a number of antennas are deployed in a fixed constrained area, there exists a trade-off between M and d, and it is important to analyze the effect of mutual coupling on the achievable receive diversity gain of the massive MIMO systems [6].

Firstly, with fixed antenna spacing, the antenna number receives diversity gain GM is defined as follows [6].

$$\mathbb{G}_M=\mathcal{E}_M^{dmin}-\mathcal{E}_{Mmin}^{dmin} \tag{41}$$

where $\mathbb{G}_M$ is the antenna number receive diversity gain, $\mathcal{E}_M^{dmin}$ is the expectation

of the received SNR at the user end (UE) with M antenna, and minimum antenna spacing distance $dmin$ at the antenna array of the BS, and $\mathcal{E}_{Mmin}^{dmin}$ is the expectation of the received SNR at UE with minimum number of antenna elements $Mmin$ and minimum distance spacing at the antenna array of the BS [6].

In another case with a fixed number of antenna elements at the BS, the antenna spacing receive diversity gain $\mathbb{G}_d$ is defined as follows [6].

$$\mathbb{G}_d = \mathcal{E}_{Mmin}^{d} - \mathcal{E}_{Mmin}^{dmin} \tag{42}$$

where $\mathbb{G}_d$ is the antenna spacing receive gain, $\mathcal{E}_{Mmin}^{d}$ is the expectation of the receive SNR at the UE with an antenna spacing d and $Mmin$ at the antenna array of the BS [6].

The average SNR (signal to noise ratio) seen at the UE terminal side can be written as follows.

$$SNR_{UE} = SNR_{BS} \left\| \boldsymbol{G}^{TC} \boldsymbol{G} \right\| \tag{43}$$

where $\boldsymbol{G}^{TC}$ is the conjugate transpose of $\boldsymbol{G}$ the channel fading gain, which is noted as below.

$$\boldsymbol{G} = \boldsymbol{HAKF}_{eq} \beta^{1/2} \tag{44}$$

Then with M antenna elements with antenna spacing distance d, the expectation of the SNR at UE terminal can be obtained as follows.

$$\mathcal{E}_{M}^{d} = E\left\{ SNR_{UE} \right\} \tag{45}$$

$$\mathcal{E}_{M}^{d} = E\left\{ \left\| \boldsymbol{G}^{TC} \boldsymbol{G} \right\| \right\} \tag{46}$$

$$\mathcal{E}_{M}^{d} = SNR_{BS} N \beta \left\| \boldsymbol{F}_{eq}^{TC} \boldsymbol{K}^{TC} \boldsymbol{A}^{TC} \boldsymbol{H}^{TC} \boldsymbol{HAKF}_{eq} \right\| \tag{47}$$

In which denotes $E\{.\}$ the expectation operation. The reason for using expectation operation there is a random variable or process, which is the channel matrix caused by channel fading environment [9]. Furthermore obtaining $\mathbb{G}_M$, and $\mathbb{G}_d$ through substituting Equation (47) into Equation (41), and Equation (42) and replacing d, and M with $dmin$, and $Mmin$ [6]. Assuming $dmin = 0.1\lambda$, $Mmin = 1$, and $\beta = 1$ as mentioned in [6].

5. Effective Capacity, and Spectral Efficiency Model

The maximum rate or spectral efficiency is as follows [5] [6].

$$R_{max} = \log_2 \left| \boldsymbol{I} + \frac{SNR_{BS}}{N_s} \boldsymbol{\Sigma}_{F^2} \boldsymbol{\Sigma}_{H^2} \right| \tag{48}$$

where $|.|$ is the determent operation of the matrix, with

$$\boldsymbol{\Sigma}_{F^2} = \boldsymbol{\Sigma}_F \boldsymbol{\Sigma}_F^{TC} \tag{49}$$

and

$$\boldsymbol{\Sigma}_{H^2} = \boldsymbol{\Sigma}_H^{TC} \boldsymbol{\Sigma}_H . \tag{50}$$

Spectral efficiency is equal to the effective capacity per bandwidth wide [5].

From Equation (48), the maximum available rate can be simplified as follows.

$$R_{max} = \log_2 \left| \frac{SNR_{BS}}{N_s} \left(\frac{N_s}{SNR_{BS}} \boldsymbol{I} + \boldsymbol{\Sigma}_{F^2} \boldsymbol{\Sigma}_{H^2} \right) \right| \tag{51}$$

$$R_{max} = r \log_2 \left(\frac{SNR_{BS}}{N_s} \right) + \log_2 \left(\prod_{i=1}^{r} \left(\frac{N_s}{SNR_{BS}} + f_i^2 \gamma_i^2 \right) \right) \tag{52}$$

The effective capacity under multimedia constraints can be defined as follows.

$$C_E(\theta) = \frac{-1}{\theta T} \ln \left(E \left\{ \mathrm{e}^{-\theta BTR} \right\} \right) \tag{53}$$

where θ is the QoS quality of service statistical exponent, B is the transmission bandwidth, and T is the time frame, $C_E(\theta)$ is the effective capacity where both QoS statistical exponent, and mutual coupling are evaluated. During the time frame T, the channel fading kept static. Considering the maximum available rate in Equation (52), and Equation (53) can be extended as follows.

$$C_E(\theta) = -\frac{1}{\theta T} \ln \left(E \left\{ \mathrm{e}^{-\theta TB \left(\log_2 \left(\frac{SNR_{BS}}{N_S} \right) + \log_2 \left(\prod_{i=1}^{r} \left(\frac{N_s}{SNR_{BS}} + f_i^2 \gamma_i^2 \right) \right) \right)} \right\} \right) \tag{54}$$

$$C_E(\theta) = -\frac{1}{\theta T} \ln \left(\mathrm{e}^{-\theta TB \log_2 \left(\frac{SNR_{BS}}{N_S} \right)} E \left\{ \left(\mathrm{e}^{\log_2 \left(\prod_{i=1}^{r} \left(\frac{N_s}{SNR_{BS}} + f_i^2 \gamma_i^2 \right) \right)} \right)^{-\theta TB} \right\} \right) \tag{55}$$

$$C_E(\theta) = -\frac{1}{\theta T} \ln \left(\mathrm{e}^{-\theta TB \log_2 \left(\frac{SNR_{BS}}{N_S} \right)} E \left\{ \left(\prod_{i=1}^{r} \left(\frac{N_s}{SNR_{BS}} + f_i^2 \gamma_i^2 \right) \right)^{\frac{-\theta TB}{\ln(2)}} \right\} \right) \tag{56}$$

From the above equations, that is clearly a convex function. Then the upper bound of the effective capacity can be obtained using Jensen's inequality [6].

$$C_E(\theta) = \frac{-1}{\theta T} \ln \left(E \left\{ \mathrm{e}^{-\theta BTR} \right\} \right) \tag{57}$$

$$C_E(\theta) \le \frac{-1}{\theta T} \ln \left(E \mathrm{e}^{-\theta BTE\{R\}} \right) \tag{58}$$

$$C_E(\theta) \le BE\{R\} \tag{59}$$

From Equation (52) $E\{R_{max}\}$ can be expressed as follows.

$$E\{R_{max}\} = E \left\{ r \log_2 \left(\frac{SNR_{BS}}{N_s} \right) + \log_2 \left(\prod_{i=1}^{r} \left(\frac{N_s}{SNR_{BS}} + f_i^2 \gamma_i^2 \right) \right) \right\} \tag{60}$$

$$E\{R_{max}\} \le r \log_2 \left(\frac{SNR_{BS}}{N_s} \right) + \sum_{i=1}^{r} \log_2 \left(E \left\{ \frac{N_s}{SNR_{BS}} + f_i^2 \gamma_i^2 \right\} \right) \tag{61}$$

$$E\{R_{max}\} \le r \log_2 \left(\frac{SNR_{BS}}{N_s} \right) + \sum_{i=1}^{r} \log_2 \left(\frac{N_s}{r} E \left\{ \gamma_i^2 N_s + \gamma_i^2 \frac{\sum_{i=1}^{r} \frac{1}{\gamma_i^2}}{SNR_{BS}} \right\} \right) \tag{62-a}$$

$$E\{R_{max}\} \le r\log_2\left(\frac{SNR_{BS}}{N_s}\right) + \sum_{i=1}^{r}\log_2\left(\frac{N_s}{r^2}\left(N_s + \frac{r}{SNR_{BS}}\right)E\left\{\sum_{i=1}^{r}\gamma_i^2\right\}\right) \quad (62\text{-b})$$

$$E\{R_{max}\} \le r\log_2\left(\frac{SNR_{BS}}{N_s}\right) + \sum_{i=1}^{r}\log_2\left(\frac{N_s}{r^2}\left(N_s + \frac{r}{SNR_{BS}}\right)E\left\{tr\left(\boldsymbol{H}^{TC}\boldsymbol{HAKK}^{TC}\boldsymbol{A}^{TC}\right)\right\}\right) \quad (63)$$

$$E\{R_{max}\} \le r\log_2\left(\frac{SNR_{BS}}{N_s}\right) + \sum_{i=1}^{r}\log_2\left(\frac{N_s}{r^2}\left(N_s + \frac{r}{SNR_{BS}}\right)\left(tr\left(\boldsymbol{AKK}^{TC}\boldsymbol{A}^{TC}\right) + E\left\{tr\left(\boldsymbol{HH}^{TC}\right)\right\}\right)\right) \quad (64)$$

Wishart Matrices is defined as follows [16].

$$\boldsymbol{W} = \boldsymbol{HH}^{TC} \quad (65)$$

where $\boldsymbol{H} \in \mathbb{C}^{N\times P}$, a collection number of properties of central and noncentral Wishart matrices and in some cases, their inverses are mentioned in [16]. Considering the first moments of a central Wishart matrix and its inverse referred in Lemma 2.9, and Lemma 2.10 assuming $P > r$, where $r = N$ [16].

$$E\left\{tr\left(\boldsymbol{HH}^{TC}\right)\right\} = Pr \quad (66)$$

$$E\left\{tr\left(\boldsymbol{W}^{-1}\right)\right\} = \frac{r}{P-r} \quad (67)$$

$$C_E(\theta) \le B\left(r\log_2\left(\frac{SNR_{BS}}{N_s}\right) + \sum_{i=1}^{r}\log_2\left(\frac{N_s}{r^2}\left(N_s + \frac{r}{SNR_{BS}}\right)\left(tr\left(\boldsymbol{AKK}^{TC}\boldsymbol{A}^{TC}\right) + Pr\right)\right)\right) \quad (68)$$

$$C_{upper}(\theta) = B\left(r\log_2\left(\frac{SNR_{BS}}{N_s}\right) + \sum_{i=1}^{r}\log_2\left(\frac{N_s}{r^2}\left(N_s + \frac{r}{SNR_{BS}}\right)\left(tr\left(\boldsymbol{AKK}^{TC}\boldsymbol{A}^{TC}\right) + Pr\right)\right)\right) \quad (69)$$

$$Spef_{max} = \left(r\log_2\left(\frac{SNR_{BS}}{N_s}\right) + \sum_{i=1}^{r}\log_2\left(\frac{N_s}{r^2}\left(N_s + \frac{r}{SNR_{BS}}\right)\left(tr\left(\boldsymbol{AKK}^{TC}\boldsymbol{A}^{TC}\right) + Pr\right)\right)\right) \quad (70)$$

where R_{max} is the maximum available rate, which is as same as $Spef_{max}$, $Spef_{max}$ is the maximum spectral efficiency, $C_E(\theta)$, and $C_{upper}(\theta)$ are both the upper bound of effective capacity, P is the number of incidents scattering directions, r is the rank of small-scale fading scattering matrix $\boldsymbol{H}$, and $tr()$ is the trace operation of matrix.

Based on Equation (52) the upper bound of the maximum available rate is derived in Equation (62), considering the simplification of Lemma 2.9 in [6] [16]. The upper bound of the effective capacity is finally expressed in Equation (69). Finally, the maximum spectral efficiency or upper bound of spectral efficiency is expressed in Equation (70). The improvement of the mutual coupling effect on

the performance of the 5G massive MIMO is accomplished by reducing the mutual coupling, which has now reached 87.5%, as mentioned in [17]. It is possible to improve the performance partially by calibrating the mutual coupling in the digital domain. However, the simple and effective approach is to use the techniques such as defected ground structure, parasitic or slot element, complementary split ring resonator, and decoupling networks which can overcome the mutual coupling effects by means of physical implementation [18].

6. Numerical Simulation and Results

The simulation using MATLAB program release 2021 is performed. The performance of multimedia constraints oriented massive MIMO technique is demonstrated, in terms of receive diversity gain both antenna number and antenna spacing, upper bound of spectral efficiency, maximum or upper bound of effective capacity, number of scattering directions effects, and effect of QoS (Quality of Service) statistical exponent. The program first creates a random matrix of scattering media and steering matrix, then computes the mutual coupling matrix with different antenna numbers and spacing distance. After this procedure the programs compute the equivalent channel matrix and precoding matrix. Then every program computing the desired performance, such as upper bound of effective capacity using Equation (69), maximum spectral efficiency using Equation (70), antenna spacing distance receive diversity gain using Equation (42), and antenna number receive diversity gain using Equation (41). The QoS statistical exponent effect on the effective capacity is accomplished using Equation (56) with terms of Equations (69). The reasonable minimum antenna spacing distance $dmin = 0.1\lambda$, the minimum antenna number $Mmin = 1$, the large-scale fading coefficient $\beta = 1$, the load impedance $Z_L = 50\,\Omega$ and the antenna dimension or the dipole length $h = 0.5\lambda$ with frame duration time $T = 1$ msec.

Results from these programs are summarized as follows. **Figure 2** shows the effects of the distance between two elements of the antenna array, which is measured by the ratio of the wavelength, on the real part (resistance), and imaginary part (reactance) of the mutual coupling impedance. **Figure 3** shows the effects of the distance between two elements of the antenna array, which is measured by the ratio of the wavelength, on the upper bound of the effective capacity. **Figure 4** shows the effects of the distance between two adjacent elements of the antenna array, which is measured by the ratio of the wavelength, of total elements number is equal to 900 elements with 100 independent incident directions, the number of data streams is equal to 4, and number of the antenna elements at the receiver terminal mobile is equal to two antennas, on the upper bound of spectral efficiency. From **Figure 5**. shows the affection on antenna number receives diversity gain at the receiver terminal with respect to the number of the antenna elements considering different of signal to noise ratio levels of the base station. The graph in **Figure 6** shows the effects of the Antenna spacing distance between elements on the antenna spacing distance receive gain at different signal-to-noise ratios. **Figure 7**

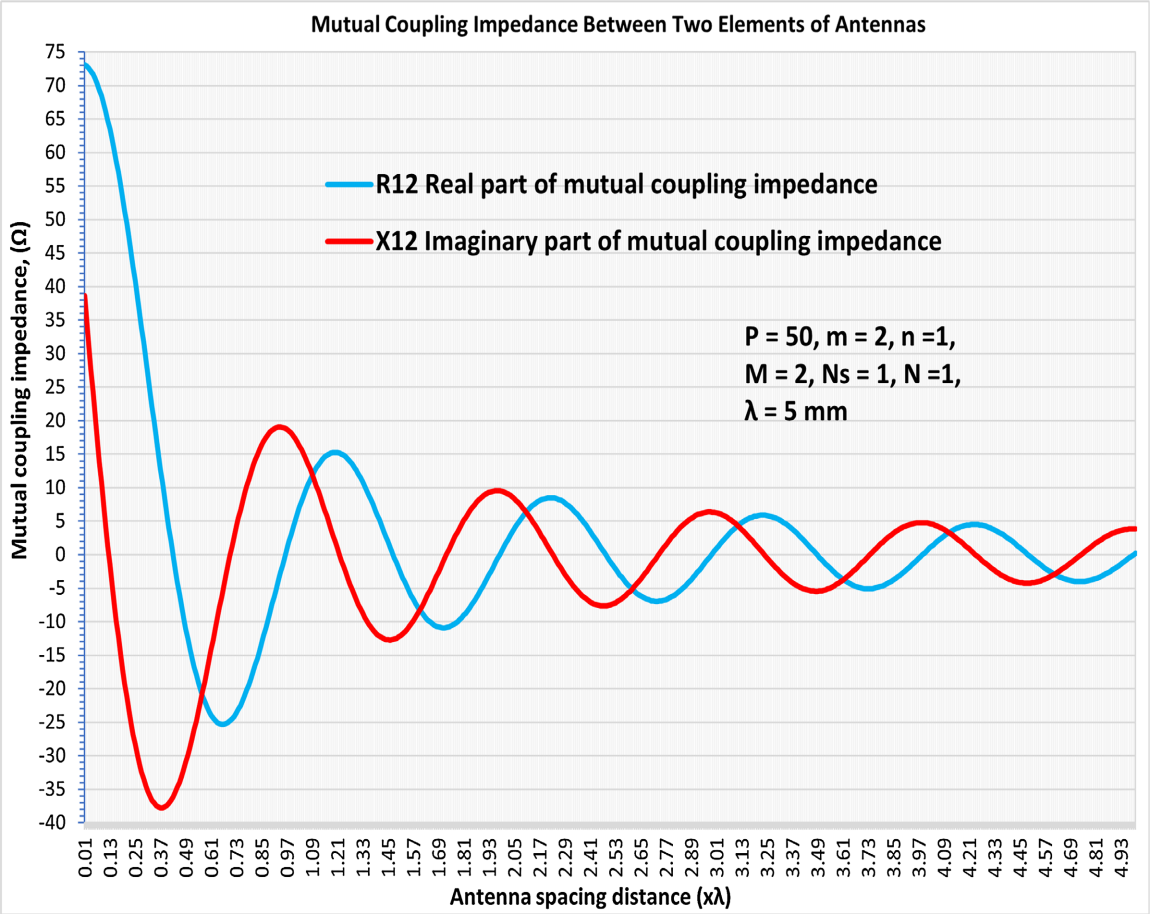

Figure 2. Mutual coupling impedance versus antenna spacing distance.

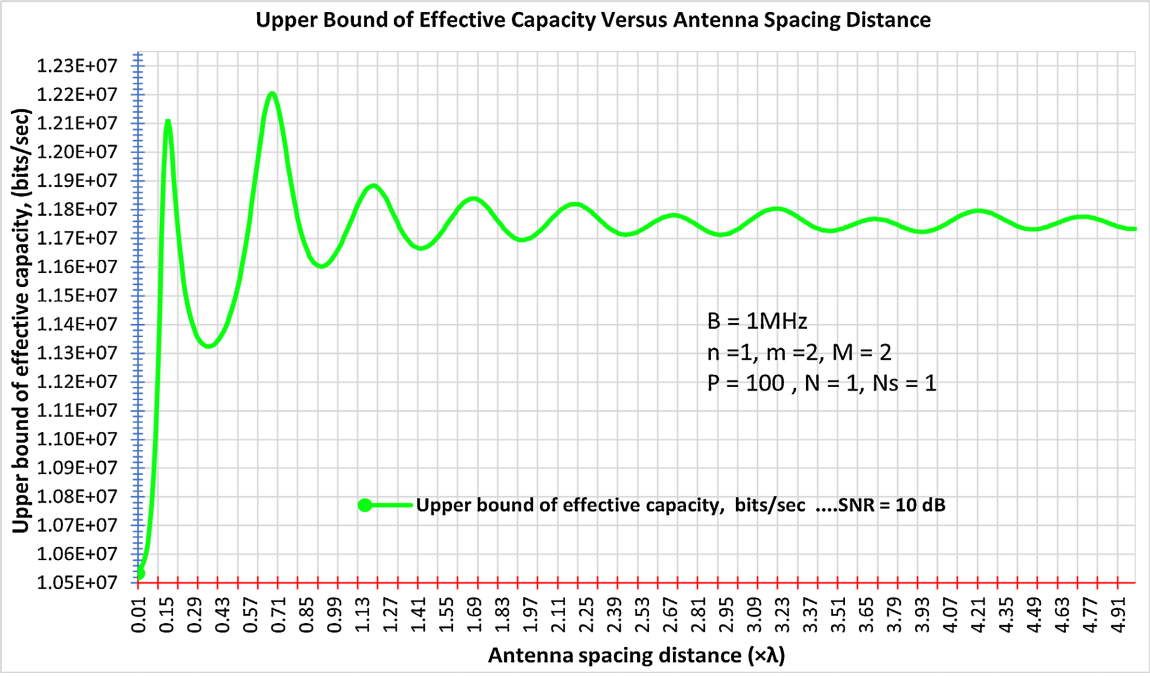

Figure 3. Upper bound of effective capacity with respect to the antenna spacing distance.

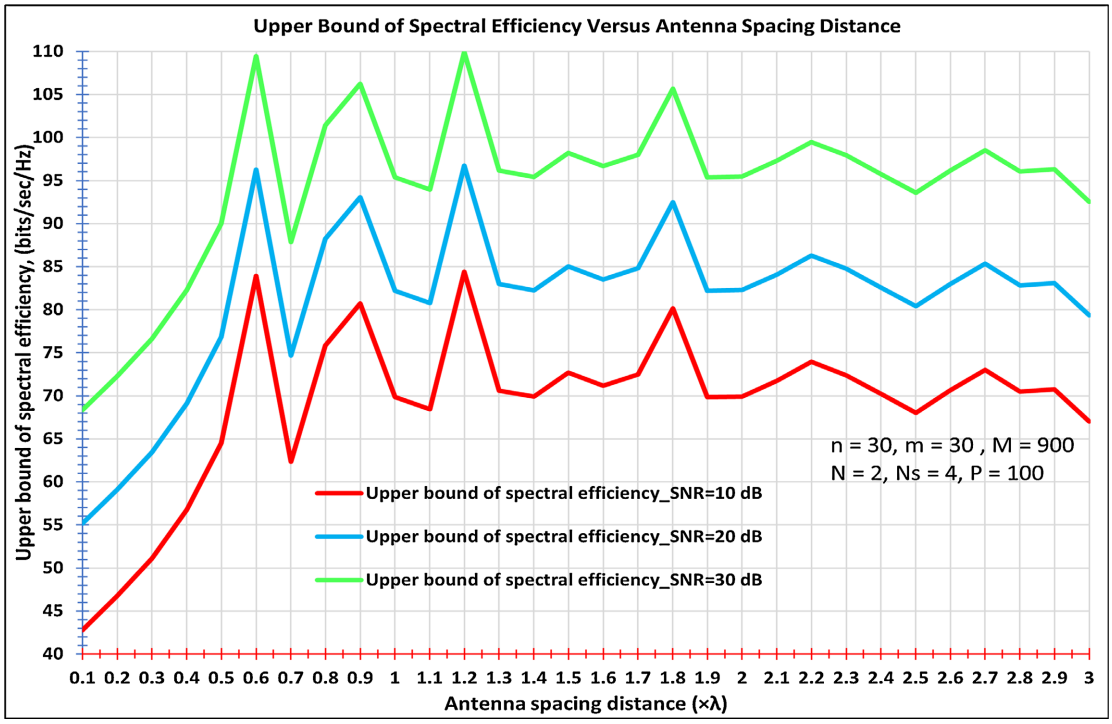

Figure 4. Upper bound of spectral efficiency with respect to the antenna spacing distance considering different signal to noise ratio level of the base station.

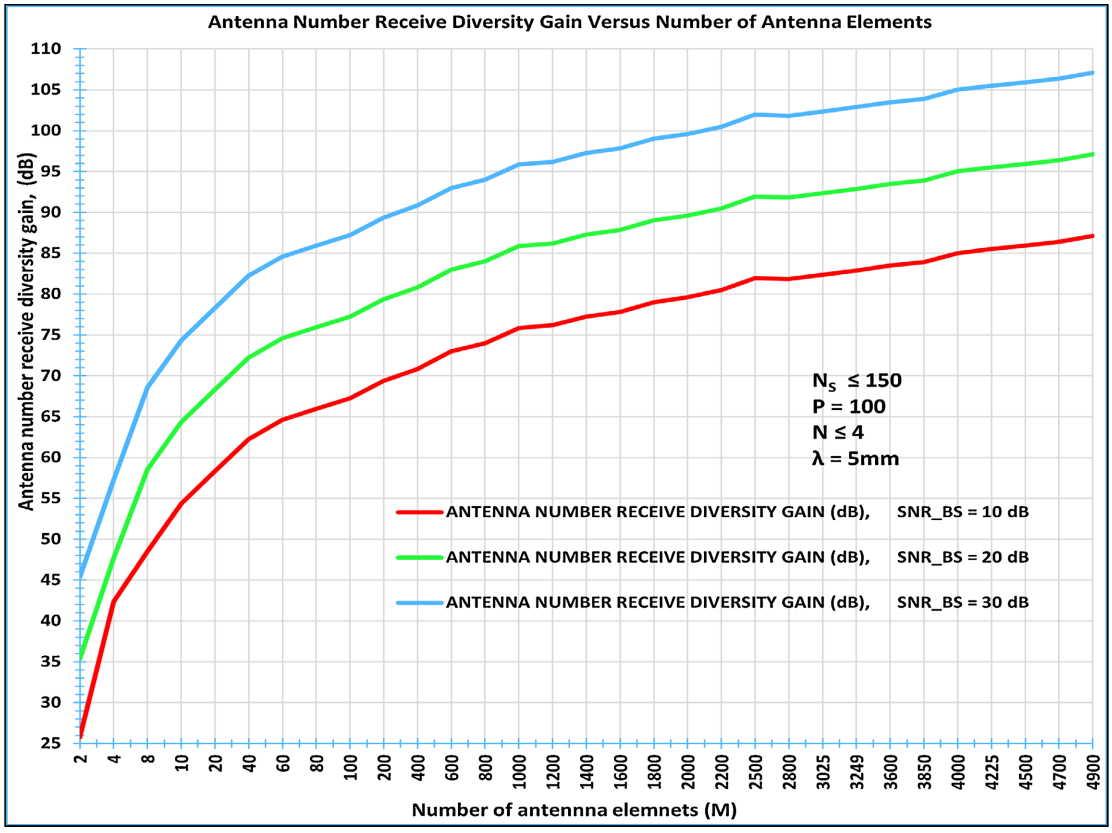

Figure 5. Antenna number receive diversity gain with respect to the number of antenna elements considering different of signal to noise ratio level of the base station.

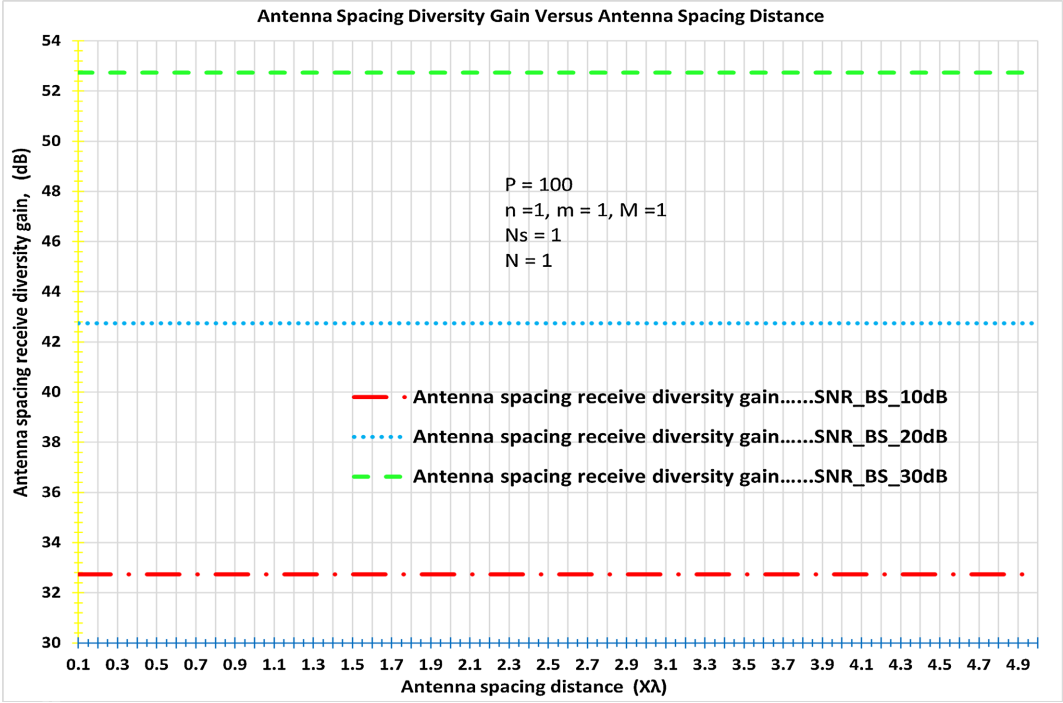

Figure 6. Antenna spacing receives diversity gain with respect to the antenna spacing distance considering different signal to Nois ratio level of the base station.

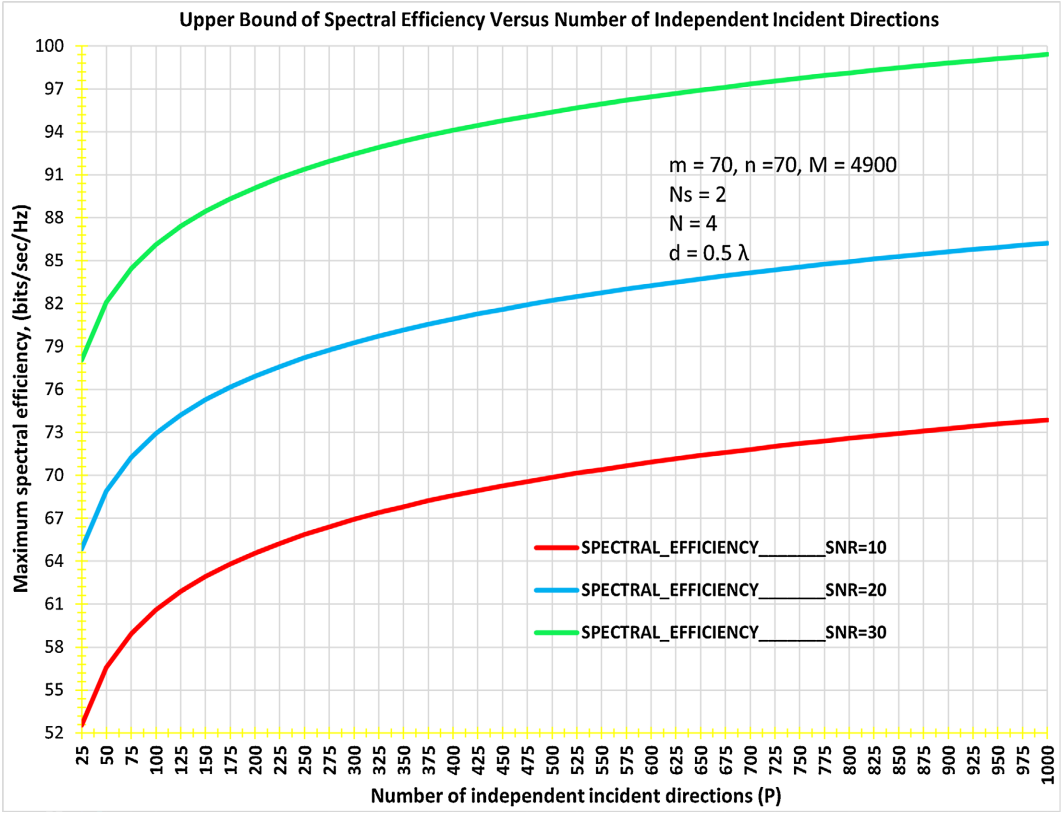

Figure 7. Maximum spectral efficiency versus number of independent incident direction with considering different signal to Noise ratio level of the base station.

illustrates the correlation between the spectral efficiency and the number of independent incident directions. Figure 8 illustrates the correlation between the spectral efficiency and the number of antenna elements at different signal-to-noise ratios. Figure 9 illustrates the effects of QoS statistical exponent on the effective capacity at different signal-to-noise ratios. Figure 10 illustrates the best performance produced when the mutual coupling reduction reaches 99% and above, which produces approximately a unity matrix of coupling. The shortcomings and degradation of spectral efficiency caused by mutual coupling in the wireless channels are compensated, and covered by refractions, reflections, and scattering from scattering media environment to appear at an acceptable value, which is known as a multiple path between transmitter and receivers. In addition to the huge number of elements of antenna array at the base station, and end-user mobile produce high traffic performance.

7. Conclusion

Based on the mutual coupling effect on the mutual impedance, the effective capacity, and spectral efficiency are analyzed and plotted. Results show the mutual coupling impedance variation with respect to the spacing distance of elements,

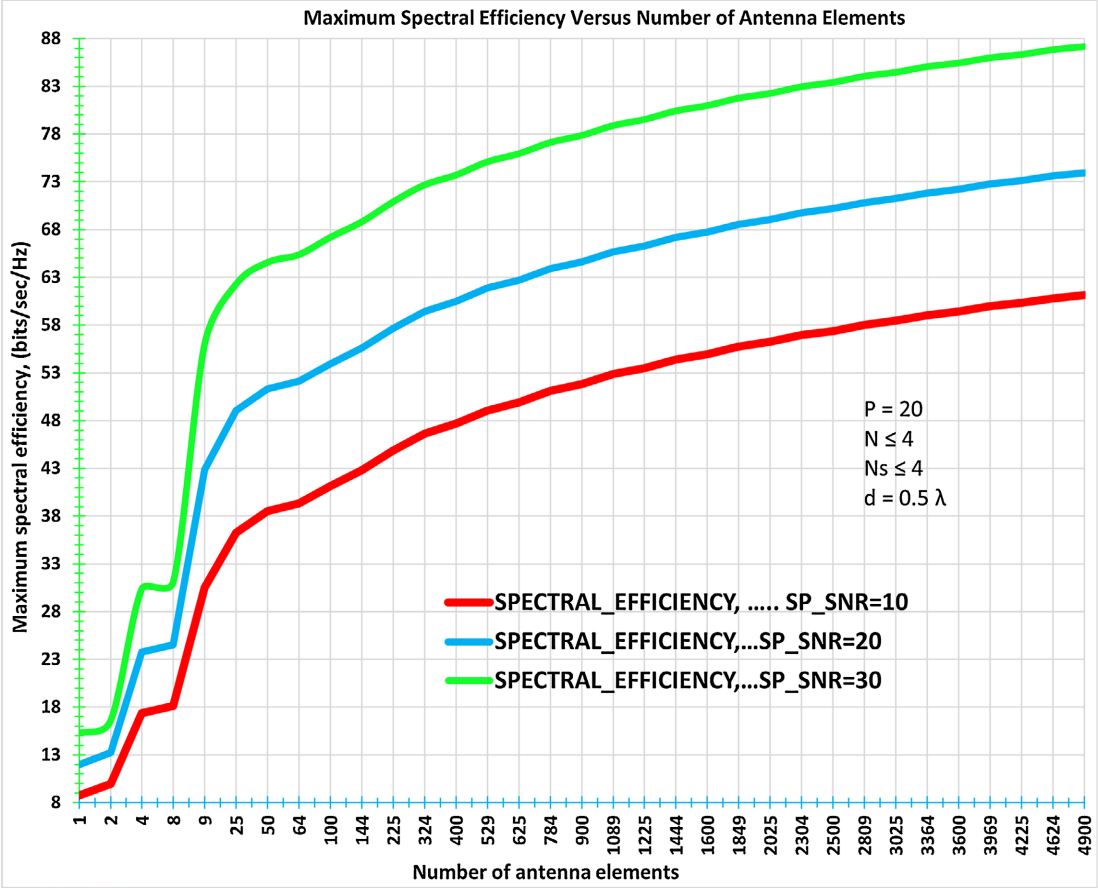

Figure 8. Maximum spectral efficiency versus number of antenna elements with considering various of signal to noise ratio level of the base station.

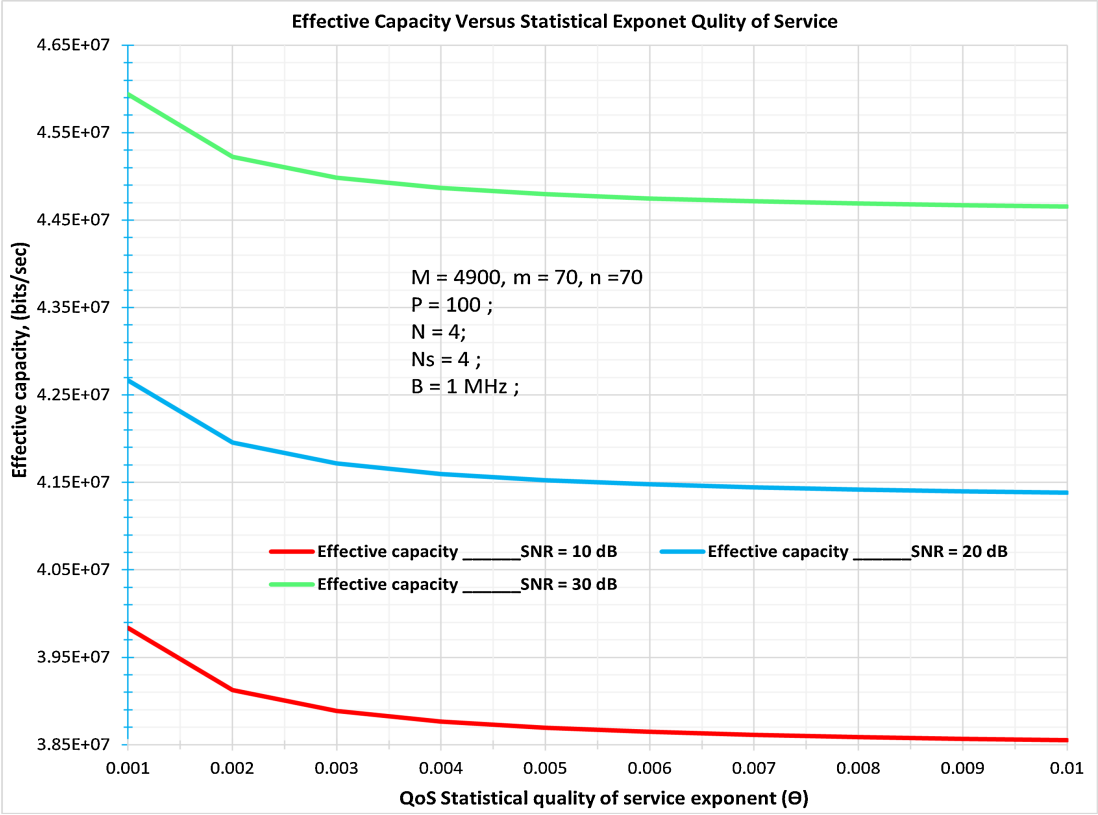

Figure 9. Effective capacity respect to the QoS statistical exponent with considering different signal to ratio levels of the base station.

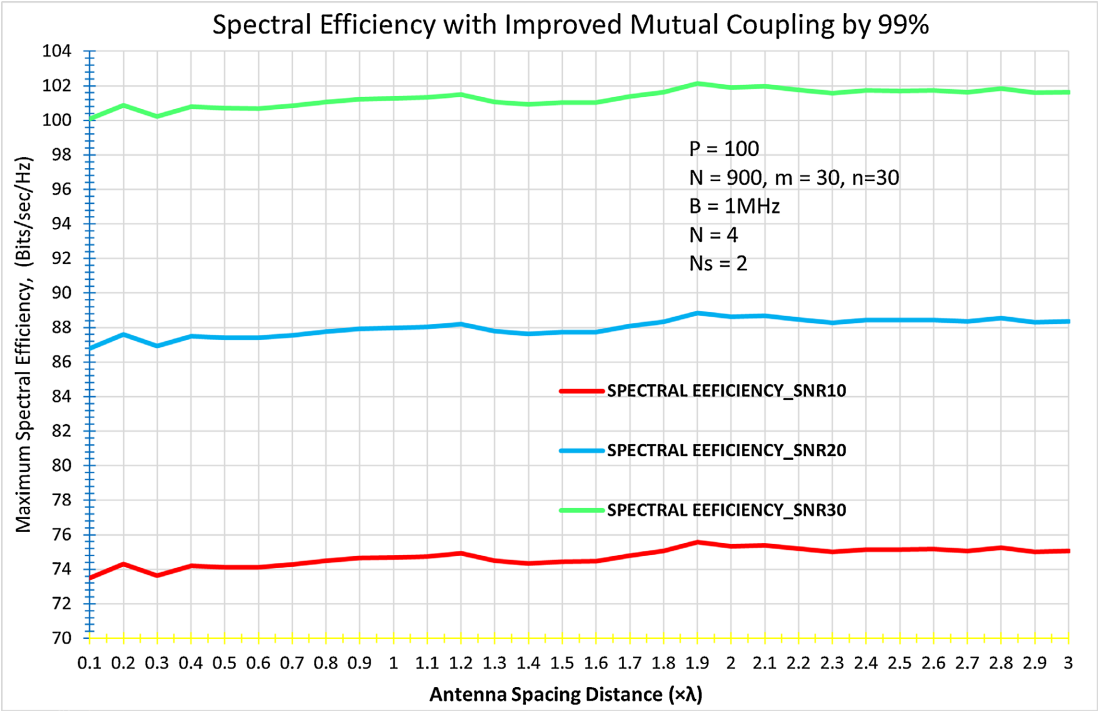

Figure 10. The upper bound of spectral efficiency with respect to the antenna spacing distance considering different signal-to-noise ratio level of the base station and improved mutual coupling impedance.

which are point to instability in the short spacing distance and kept at a small variation in effective capacity at the large spacing distance between elements. The mutual coupling effect on the maximum spectral efficiency instability on a short range of spacing distance and small dynamic variations on the large spacing distance kept at a small nonstationary on the array elements, in addition when increasing signal-to-noise ratio levels at the base station the traffic increase and variations kept at small nonstationary. The received gain is affected by the number of antenna elements of the base station, which indicates a positive correlation between the received gain and the number of antenna elements of the base station and terminal. When the number of elements at the receiver terminal increases, the received gain increases in step-up values. The received gain is not affected by mutual coupling. Results point to the positive correlation between the number of random independent incident directions with the number of elements at the base station, in addition to the number of elements at the receiver terminal, and spectral efficiency. When the QoS exponent is increased, the effective capacity will be decreased. In general, the massive MIMO mm-wave should have a high gain amplifier, which provides a higher signal-to-ratio against path loss at higher frequencies and improves traffic performance. Many techniques in the fabrication and design of antenna elements are performed to reduce the effect of mutual coupling. Improvement of the mutual coupling reached about 87%, but affection still appears. The ideal improvement is about 99%, but it is not reached today. The reduction of mutual coupling of 99% theoretically kept effective capacity, and spectral efficiency at stationary of best performance. In future work, taking into account the QoS statistical exponent constraints, a more efficient signal detection precoding algorithm enhances the results towards better performance of the multimedia massive MIMO communication systems.

Acknowledgements

The work in this paper is supported by the full Professor Mohammed Elmusrati from Vassa University Finland, and the full Professor Xiaohu Ge from the School of Electronic Information and Communications at Huazhong University of Science and Technology (HUST), China.

Conflicts of Interest

The author declares no conflicts of interest regarding the publication of this paper.

References

[1] Allen, J.L. and Diamond, B.L. (1966) Mutual Coupling in Array Antennas. Massachoutes US. Lincoln Laboratory. Technical Report 424.

[2] Dicandia, F.A. and Genovesi, S. (2021) Spectral Efficiency Improvement of 5G Massive MIMO Systems for High-Altitude Platform Stations by Using Triangular Lattice Arrays. *Sensors*, **21**, Article 3202. https://doi.org/10.3390/s21093202

[3] Mahabub, A., Rahman, M., Al-Amin, M., Rahman, M. and Rana, M. (2018) Design

of a Multiband Patch Antenna for 5G Communication Systems. *Open Journal of Antennas and Propagation*, **6**, 1-14.

[4] Jervase-Yak, J. and Al-Shamsi, A.H. (2016) MIMO Antenna for UWB Communications. *International Journal of Communications, Network and System Sciences*, **9**, 177-183. https://doi.org/10.4236/ijcns.2016.95017

[5] Koivo, H. and Elmusrati, M. (2009) Systems Engineering in Wireless Communications. Wiley. https://doi.org/10.1002/9780470021804

[6] Ge, X., Wang, H., Zi, R., Li, Q. and Ni, Q. (2016) 5G Multimedia Massive MIMO Communications Systems. *Wireless Communications and Mobile Computing*, **16**, 1377-1388. https://doi.org/10.1002/wcm.2704

[7] Gupta, I. and Ksienski, A. (1983) Effect of Mutual Coupling on the Performance of Adaptive Arrays. *IEEE Transactions on Antennas and Propagation*, **31**, 785-791. https://doi.org/10.1109/tap.1983.1143128

[8] Speyer, J.L. and Chung, W.H. (2008) Stochastic Processes, Estimation, and Control. Society for Industrial and Applied Mathematics. https://doi.org/10.1137/1.9780898718591

[9] Magnus, J.R. and Magnus, J.R. (2019) Matrix Differential Calculus with Applications in Statistics and Econometrics. Wiley. https://doi.org/10.1002/9781119541219

[10] Shen, S., McKay, M.R. and Murch, R.D. (2010) MIMO Systems with Mutual Coupling: How Many Antennas to Pack into Fixed-Length Arrays? 2010 *International Symposium on Information Theory & Its Applications*, Taichung, 17-20 October 2010, 531-536. https://doi.org/10.1109/isita.2010.5654383

[11] Harold, M. and McQuiddy, D.N. (1965) Mutual Impedance Effect on Scanned Antenna Array. Technical Report No.2. Contrast NAS8-11295.

[12] Schelkunoff Sergei, A. and Friis Harald, T. (1952) Antennas Theory and Practice. John Wiley & Sons.

[13] Balanis Constantine, A. (2005) Antenna Theory Analysis and Design. 3rd Edi-tion, John Wiley & Sons.

[14] Jordan Edward, C. & Balmain Keith, G. (1968) Electromagnetic Waves and Radiating Systems. 2nd Edition, Prentice-Hall.

[15] Zhang, E. and Huang, C. (2014) On Achieving Optimal Rate of Digital Precoder by Rf-Baseband Codesign for MIMO Sysftems. 2014 *IEEE* 80*th Vehicular Technology Conference* (*VTC*2014-*Fall*), Vancouver, 14-17 September 2014, 1-5. https://doi.org/10.1109/vtcfall.2014.6966076

[16] Tulino, A.M. and Verdú, S. (2004) Random Matrix Theory and Wireless Communications. Now Publishers Inc. https://doi.org/10.1561/9781933019505

[17] Nassar, M.A., Soliman, H.Y., Abdallah, R.M. and Abdallah, E.A.F. (2023) Improving Mutual Coupling in MIMO Antennas Using Different Techniques. *Progress In Electromagnetics Research C*, **133**, 81-95. https://doi.org/10.2528/pierc23033106

[18] Nadeem, I. and Choi, D. (2019) Study on Mutual Coupling Reduction Technique for MIMO Antennas. *IEEE Access*, **7**, 563-586. https://doi.org/10.1109/access.2018.2885558